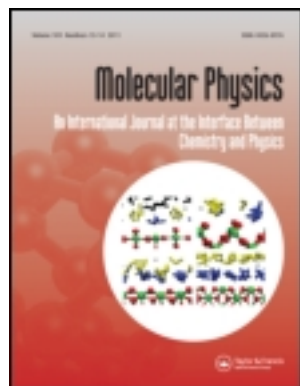


This article was downloaded by: [Stanford University]

On: 13 July 2013, At: 10:52

Publisher: Taylor & Francis

Informa Ltd Registered in England and Wales Registered Number: 1072954 Registered office: Mortimer House, 37-41 Mortimer Street, London W1T 3JH, UK



Molecular Physics: An International Journal at the Interface Between Chemistry and Physics

Publication details, including instructions for authors and subscription information:

<http://www.tandfonline.com/loi/tmph20>

Dependence of diatomic photofragment fluorescence polarization on triatomic predissociation lifetime

Gary W. Loge^a & Richard N. Zare^b

^a Department of Chemistry, Cornell University, Ithaca, New York, 14853, U.S.A.

^b Department of Chemistry, Stanford University, Stanford, California, 94305, U.S.A.

Published online: 23 Aug 2006.

To cite this article: Gary W. Loge & Richard N. Zare (1981) Dependence of diatomic photofragment fluorescence polarization on triatomic predissociation lifetime, *Molecular Physics: An International Journal at the Interface Between Chemistry and Physics*, 43:6, 1419-1428, DOI: [10.1080/00268978100102171](https://doi.org/10.1080/00268978100102171)

To link to this article: <http://dx.doi.org/10.1080/00268978100102171>

PLEASE SCROLL DOWN FOR ARTICLE

Taylor & Francis makes every effort to ensure the accuracy of all the information (the "Content") contained in the publications on our platform. However, Taylor & Francis, our agents, and our licensors make no representations or warranties whatsoever as to the accuracy, completeness, or suitability for any purpose of the Content. Any opinions and views expressed in this publication are the opinions and views of the authors, and are not the views of or endorsed by Taylor & Francis. The accuracy of the Content should not be relied upon and should be independently verified with primary sources of information. Taylor and Francis shall not be liable for any losses, actions, claims, proceedings, demands, costs, expenses, damages, and other liabilities whatsoever or howsoever caused arising directly or indirectly in connection with, in relation to or arising out of the use of the Content.

This article may be used for research, teaching, and private study purposes. Any substantial or systematic reproduction, redistribution, reselling, loan, sub-licensing, systematic supply, or distribution in any form to anyone is expressly forbidden. Terms & Conditions of access and use can be found at <http://www.tandfonline.com/page/terms-and-conditions>

Dependence of diatomic photofragment fluorescence polarization on triatomic predissociation lifetime

by GARY W. LOGE

Department of Chemistry, Cornell University, Ithaca,
New York, 14853, U.S.A.

and RICHARD N. ZARE

Department of Chemistry, Stanford University, Stanford,
California 94305, U.S.A.

(Received 17 March 1981 ; accepted 26 April 1981)

When a triatomic molecule, ABC , is dissociated by a beam of light to yield an electronically excited diatomic molecule, AB^* , the degree of linear polarization of the AB^* photofragment fluorescence depends in general on the lifetime of the excited parent molecule, ABC^* . Analytical expressions are developed for the polarization of diatomic fluorescence as a function of predissociation lifetime. These calculations are carried out under the assumptions that: (a) the absorption and emission transition dipole moments can be replaced by classical hertzian dipole oscillators; (b) the AB^* fragment rotates in the plane of the ABC^* parent at the time of dissociation; and (c) the motion of the ABC^* parent can be approximated by the classical motion of a prolate or oblate symmetric top.

1. INTRODUCTION

Photodissociation dynamics can be studied readily in those photoprocesses resulting in the formation of electronically excited fragments by examining the nature of the subsequent fluorescence. For example, an analysis of the fluorescence spectrum as a function of excitation wavelength reveals the disposal of energy in the dissociation process [1, 2], while a measurement of the degree of polarization of the atomic [3, 4] or molecular [5-12] fluorescence may determine the symmetry nature of the repulsive state from which dissociation precedes. A previous paper [10] considered the degree of polarization of the AB^* excited diatomic photofragment when a triatomic molecule ABC is photolyzed by a beam of light. In that treatment several assumptions were made:

- (1) the AB^* radiative lifetime is sufficiently short so that the fluorescence occurs under essentially collision-free conditions at pressures of the parent molecule that allow measurable fluorescence signals;
- (2) the absorption and emission process may be described by classical hertzian dipole oscillators;
- (3) the parent rotational angular momentum may be neglected relative to the diatomic fragment rotational angular momentum;
- (4) the excited parent molecule falls apart directly so that it has no time to rotate before dissociating.

The third assumption considerably simplifies the calculation of the degree of polarization when the excited parent molecule is planar. Because the interactions of all sub-parts of the parent are directed in the plane of the molecule, the torque exerted on the AB^* fragment by the departing fragment C must be such that it causes the AB^* molecule to rotate in the plane of the parent molecule at the time of dissociation. The fourth assumption further simplifies the calculation in that a knowledge of the initial orientation of the excited parent molecule is all that is needed to calculate the degree of polarization.

In the present work this last assumption is relaxed. Instead, we suppose that ABC^* dissociates at a constant rate so that its population decreases to $1/e$ of its original value in a time τ ; we call τ the predissociation lifetime. As we shall see, the effect of lengthening the predissociation lifetime is always in the direction of decreasing the observed degree of polarization, although there are certain cases where the degree of polarization is unaffected by predissociation.

2. CALCULATION OF THE PHOTOFRAGMENT FLUORESCENCE POLARIZATION

Traditionally, polarization measurements are carried out using a perpendicular excitation/detection geometry [13]. The fluorescence intensity polarized parallel and perpendicular to the polarization vector of the incident light beam is denoted by I_{\parallel} and I_{\perp} , respectively. Then the degree of polarization, P , is defined by

$$P = (I_{\parallel} - I_{\perp}) / (I_{\parallel} + I_{\perp}) \quad (1)$$

and the polarization anisotropy, R , by

$$R = (I_{\parallel} - I_{\perp}) / (I_{\parallel} + 2I_{\perp}). \quad (2)$$

Note that $P = 3R / (2 + R)$ so that knowledge of one implies knowledge of the other.

In the classical high J limit, the electric dipole transition moment of the molecule may be replaced by a hertzian dipole oscillator, μ , pointing in the same direction and attached rigidly to the molecular framework. Let the absorption and emission oscillators be denoted by μ_{abs} and μ_{em} . We define the average square of the cosine of the angle between μ_{abs} and μ_{em} by $\langle \cos^2 \gamma \rangle$. Then it may be shown [13, 14] that the polarization parameters, P and R , can be rewritten in terms of $\langle \cos^2 \gamma \rangle$:

$$P = [3\langle \cos^2 \gamma \rangle - 1] / [\langle \cos^2 \gamma \rangle + 3] \quad (3)$$

and

$$\begin{aligned} R &= [3\langle \cos^2 \gamma \rangle - 1] / 5, \\ &= \frac{2}{5} \langle P_2(\cos \gamma) \rangle. \end{aligned} \quad (4)$$

Thus P or R can be determined once $\langle \cos^2 \gamma \rangle$ has been calculated. This assumes a beam of linearly polarized light causes dissociation. If the light beam is unpolarized then a reduced degree of polarization $P' = -P / (2 - P)$ results [13], where I_{\parallel} and I_{\perp} refer to the fluorescence intensities parallel and perpendicular to the unpolarized light beam.

We find $\cos^2 \gamma$ by taking the appropriate time weighted average of $\cos^2 \gamma(t) = |\hat{\mu}_{\text{abs}}(0) \cdot \hat{\mu}_{\text{em}}(t)|^2$, i.e.

$$\begin{aligned} \cos^2 \gamma &= \int_0^\infty \cos^2 \gamma(t) \exp(-t/\tau) d(t/\tau), \\ &= \mathcal{L}\{\cos^2 \gamma(t)\}. \end{aligned} \tag{5}$$

In general, $\hat{\mu}_{\text{em}}$ may have a spatial distribution due to the rotation of the AB^* fragment. An appropriate average over this distribution must be included in the calculation of $\cos^2 \gamma$. In addition, we must average over all initial orientations of the ABC^* molecule to form the ensemble average

$$\langle \cos^2 \gamma \rangle = [\mathcal{L}\{\cos^2 \gamma(t)\}]_{\text{av}}. \tag{6}$$

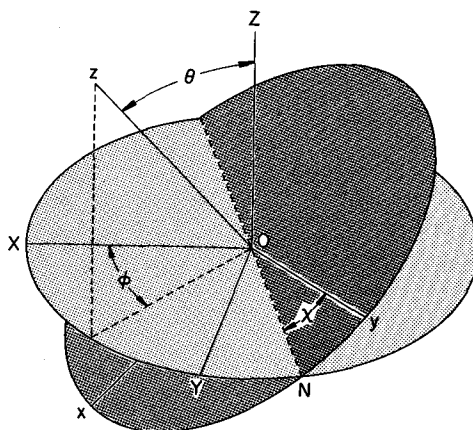


Figure 1. The Euler angles, ϕ , θ , χ , relating the laboratory frame $F=XYZ$ and the body-fixed frame $g=xyz$ with the common origin O . The XY and xy planes intersect along the lines of nodes, ON .

Let the ABC^* molecule be approximated by a symmetric top. We denote the figure axis by z and the total angular momentum by \mathbf{J} . At any instant, the principal axes can be described relative to \mathbf{J} (chosen to be along the Z axis) by the three Euler angles, ϕ , θ , χ , defined in figure 1. Here θ describes the angle z makes with Z ; ϕ describes the precession of the figure axis about $\mathbf{J}(Z)$; and χ describes the rotation of the top about its own figure axis (z). For a symmetric top [15]

$$\left. \begin{aligned} \dot{\theta} &= 0, \\ \dot{\phi} &= J/I_x, \\ \dot{\chi} &= (J/I_z - J/I_x) \cos \theta, \end{aligned} \right\} \tag{7}$$

where $I_x = I_y$, I_z are the three moments of inertia. It follows from (7) that the angle θ , the rate of precession of the figure axis about \mathbf{J} , and the rate of precession of the top about its figure axis are all constant with time. In particular

$$\cos^2 \theta = K^2/J(J+1), \tag{8}$$

where K is the (quantized) projection \mathbf{J} makes on the figure axis.

By symmetry μ_{abs} must lie either in the plane of the non-linear ABC molecule or perpendicular to this plane. Also, μ_{abs} must be either parallel or perpendicular to the symmetric top figure axis. For the special case of a linear \rightarrow linear transition, μ_{abs} is specified only to whether it lies either along the internuclear axis of the ABC molecule or perpendicular to it. Similarly, symmetry restricts the possible directions of μ_{em} . In particular, μ_{em} lies either along the internuclear axis of the AB^* excited photofragment (\parallel -type transition) or in a plane perpendicular to the internuclear axis (\perp -type transition). Furthermore, μ_{em} lies in the rotational plane of the AB^* photofragment for a P or R transition, or μ_{em} lies perpendicular to the plane of rotation for a Q transition. All these cases are summarized in table 1.

Table 1. Different orientations of the absorption and emission hertzian dipole oscillators, μ_{abs} and μ_{em} , for the process $ABC + h\nu \rightarrow ABC^* \rightarrow AB^* + C \rightarrow AB + C + h\nu'$. The ABC^* molecule is approximated as a symmetric top and the AB^* fragment is assumed to be formed with its angular momentum \mathbf{J} perpendicular to the ABC^* plane at the time of dissociation. Between the time of absorption and dissociation the ABC^* molecule may rotate. We denote the initial orientation of the ABC^* plane by Δ and the final one by Δ' . The direction of μ_{abs} may point either along the figure axis z of the ABC^* top for a $\Delta K=0$ transition or perpendicular to z for a $\Delta K=\pm 1$ transition. In addition, μ_{abs} may lie either in the plane Δ or be perpendicular to Δ . The direction of μ_{em} is either perpendicular to the plane Δ' for a Q line ($\Delta J=0$ transition) or in the Δ' plane for an R or P line ($\Delta J=\pm 1$ transition).

Case	ABC^* top	μ_{abs}	μ_{em}
<i>A</i>	Oblate	$\parallel z, \perp \Delta$	$\perp \Delta'(Q)$
<i>B</i>	Oblate	$\parallel z, \perp \Delta$	$\parallel \Delta'(P, R)$
<i>C</i>	Oblate	$\perp z, \parallel \Delta$	$\perp \Delta'(Q)$
<i>D</i>	Oblate	$\perp z, \parallel \Delta$	$\parallel \Delta'(P, R)$
<i>E</i>	Prolate	$\parallel z, \parallel \Delta$	$\perp \Delta'(Q)$
<i>F</i>	Prolate	$\parallel z, \parallel \Delta$	$\parallel \Delta'(P, R)$
<i>G</i>	Prolate	$\perp z, \parallel \Delta$	$\perp \Delta'(Q)$
<i>H</i>	Prolate	$\perp z, \parallel \Delta$	$\parallel \Delta'(P, R)$
<i>I</i>	Prolate	$\perp z, \perp \Delta$	$\perp \Delta'(Q)$
<i>J</i>	Prolate	$\perp z, \perp \Delta$	$\parallel \Delta'(P, R)$

Note that we must distinguish whether the ABC^* molecule behaves as an oblate top ($I_x = I_y < I_z$) or a prolate top ($I_x = I_y > I_z$). Actually, the ABC^* molecule can only be a perfect symmetric top when it is linear. However, there are many cases where its behaviour is that of a near oblate or prolate top. For example, the symmetric BAB molecule is usually well approximated as a near prolate top [16].

In calculating $\cos^2 \gamma$ it is useful to introduce three reference frames: the space-fixed $F = X, Y, Z$ frame in which \mathbf{J} is along the Z axis; the body-fixed $g = x, y, z$ frame at time $t=0$ that describes the initial orientation of the excited ABC^* top; and the body-fixed $g' = x', y', z'$ frame that describes the orientation of the ABC^* top at the time of dissociation t . We choose the figure axis of the top to lie along the z axis of the body-fixed frame. The choice of the x and y

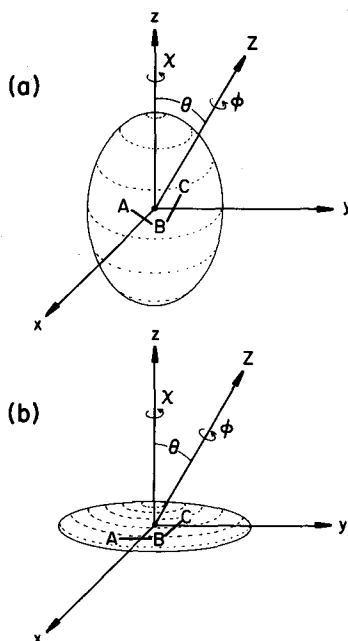


Figure 2. Moment of inertia ellipsoid for (a) a prolate symmetric top and (b) an oblate symmetric top. In both cases z is chosen to lie along the figure axis making an angle θ with respect to the total angular momentum \mathbf{J} , which lies along the Z axis of the space-fixed frame. In the prolate top the molecular plane lies in the yz plane while in an oblate top the molecular plane lies in the xy plane.

axes for a symmetric top is arbitrary. For a prolate top we choose the y axis at any time t so that y' and z' lie in the molecular plane (figure 2 (a)) while for an oblate top, x' and y' always lie in the molecular plane (see figure 2 (b)). The quantity $\cos^2 \gamma$ is calculated by identifying μ_{abs} with one of the top axes g at $t=0$ and identifying μ_{em} with one or more of the axes g' at time t . Then, according to (5)

$$\begin{aligned} \cos^2 \gamma &= \mathcal{L}\{|\hat{\mu}(0) \cdot \hat{\mu}(t)|^2\}, \\ &= \mathcal{L}\{|\hat{\mathbf{g}} \cdot \hat{\mathbf{g}}'|^2\}, \\ &= \mathcal{L}\left\{\left|\sum_F \Phi_{gF} \Phi_{Fg'}\right|^2\right\}, \end{aligned} \quad (9)$$

where Φ_{gF} and $\Phi_{Fg'}$ are the direction cosine matrix elements relating the initial body-fixed frame g to the space-fixed frame F and the frame F to the final body-fixed frame g' , respectively.

We must average $\cos^2 \gamma$ over all initial orientations of the ABC^* top to obtain $\langle \cos^2 \gamma \rangle$. Because the choice of the space-fixed X and Y axes are arbitrary, we set $\phi(0) = \phi_0 = 0$ so that z lies in the XZ plane. The average over $\chi(0) = \chi_0$ (which ranges from 0 to 2π) is equivalent to taking the average of $\cos^2 \gamma$ for $\chi_0 = 0$ and $\chi_0 = \pi/2$, since all values of χ are equally probable. Alternatively, it is more convenient to carry out the average over χ_0 by setting $\chi_0 = 0$ and taking the average of $\cos^2 \gamma$ obtained when x and y (and hence x' and

Table 2. The direction cosine matrix elements that relate the initial body-fixed frame g to the space-fixed frame F at absorption ($t=0$) and the space-fixed frame F to the final body-fixed frame g' at the time, t , of dissociation.

$$\Phi_{gF} = \begin{bmatrix} \cos \theta & 0 & -\sin \theta \\ 0 & 1 & 0 \\ \sin \theta & 0 & \cos \theta \end{bmatrix}$$

$$\Phi_{Fg'} = \begin{bmatrix} \cos \dot{\phi}t \cos \theta \cos \dot{\chi}t - \sin \dot{\phi}t \sin \dot{\chi}t & -\cos \dot{\phi}t \cos \theta \sin \dot{\chi}t - \sin \dot{\phi}t \cos \dot{\chi}t & \cos \dot{\phi}t \sin \theta \\ \sin \dot{\phi}t \cos \theta \cos \dot{\chi}t + \cos \dot{\phi}t \sin \dot{\chi}t & -\sin \dot{\phi}t \cos \theta \sin \dot{\chi}t + \cos \dot{\phi}t \cos \dot{\chi}t & \sin \dot{\phi}t \sin \theta \\ -\sin \theta \cos \dot{\chi}t & \sin \theta \sin \dot{\chi}t & \cos \theta \end{bmatrix}$$

y') are interchanged (corresponding to taking the average by placing x and then y along the line of nodes in figure 1). For this purpose (9) is evaluated using the direction cosine matrix elements given in table 2. Note that in the $\Phi_{Fg'}$, the angles $\chi(t)$ and $\phi(t)$ have been replaced by $\dot{\chi}t$ and $\dot{\phi}t$ where $\dot{\chi}$ and $\dot{\phi}$ are given by (7). In this manner $\langle \cos^2 \gamma \rangle$ is calculated for each entry appearing in table 1.

3. RESULTS AND DISCUSSION

Let us illustrate the calculation of $\langle \cos^2 \gamma \rangle$ by considering a typical example, namely, Case F of table 1. Here μ_{abs} lies along the figure axis, z , of a prolate top, and μ_{em} is in the plane of rotation of the AB^* fragment. From the choice of axes (see figure 2 (a)), μ_{em} lies equiprobably in the $y'z'$ plane, while μ_{abs} lies along z . Averaging over the rotational motion of the AB^* fragment, we find

$$\cos^2 \gamma = \frac{1}{2} [\mathcal{L}\{|\hat{\mathbf{z}} \cdot \hat{\mathbf{z}}'\|^2\} + \mathcal{L}\{|\hat{\mathbf{z}} \cdot \hat{\mathbf{y}}'\|^2\}]. \quad (10)$$

Then $\langle \cos^2 \gamma \rangle$ is found from (10) by averaging over χ_0 , i.e. by taking the average of $\cos^2 \gamma$ when x' and y' are interchanged:

$$\langle \cos^2 \gamma \rangle = \frac{1}{4} [2\mathcal{L}\{|\hat{\mathbf{z}} \cdot \hat{\mathbf{z}}'\|^2\} + \mathcal{L}\{|\hat{\mathbf{z}} \cdot \hat{\mathbf{y}}'\|^2\} + \mathcal{L}\{|\hat{\mathbf{z}} \cdot \hat{\mathbf{x}}'\|^2\}]. \quad (11)$$

In the same way $\langle \cos^2 \gamma \rangle$ is expressed in terms of the $\mathcal{L}\{|\hat{\mathbf{g}} \cdot \hat{\mathbf{g}}'\|^2\}$ for all the cases considered in table 1. The resulting expressions are displayed in table 3.

Table 3. Relation between $\langle \cos^2 \gamma \rangle$ and the $\mathcal{L}\{|\hat{\mathbf{g}} \cdot \hat{\mathbf{g}}'\|^2\}$.

Case	$\langle \cos^2 \gamma \rangle$
A	$\mathcal{L}\{ \hat{\mathbf{z}} \cdot \hat{\mathbf{z}}'\ ^2\}$
B	$\frac{1}{2} [\mathcal{L}\{ \hat{\mathbf{z}} \cdot \hat{\mathbf{x}}'\ ^2\} + \mathcal{L}\{ \hat{\mathbf{z}} \cdot \hat{\mathbf{y}}'\ ^2\}]$
C	$\frac{1}{2} [\mathcal{L}\{ \hat{\mathbf{x}} \cdot \hat{\mathbf{z}}'\ ^2\} + \mathcal{L}\{ \hat{\mathbf{y}} \cdot \hat{\mathbf{z}}'\ ^2\}]$
D	$\frac{1}{4} [\mathcal{L}\{ \hat{\mathbf{x}} \cdot \hat{\mathbf{x}}'\ ^2\} + \mathcal{L}\{ \hat{\mathbf{x}} \cdot \hat{\mathbf{y}}'\ ^2\} + \mathcal{L}\{ \hat{\mathbf{y}} \cdot \hat{\mathbf{x}}'\ ^2\} + \mathcal{L}\{ \hat{\mathbf{y}} \cdot \hat{\mathbf{y}}'\ ^2\}]$
E	$\frac{3}{4} [\mathcal{L}\{ \hat{\mathbf{z}} \cdot \hat{\mathbf{x}}'\ ^2\} + \mathcal{L}\{ \hat{\mathbf{z}} \cdot \hat{\mathbf{y}}'\ ^2\}]$
F	$\frac{1}{4} [2\mathcal{L}\{ \hat{\mathbf{z}} \cdot \hat{\mathbf{z}}'\ ^2\} + \mathcal{L}\{ \hat{\mathbf{z}} \cdot \hat{\mathbf{x}}'\ ^2\} + \mathcal{L}\{ \hat{\mathbf{z}} \cdot \hat{\mathbf{y}}'\ ^2\}]$
G	$\frac{1}{2} [\mathcal{L}\{ \hat{\mathbf{x}} \cdot \hat{\mathbf{y}}'\ ^2\} + \mathcal{L}\{ \hat{\mathbf{y}} \cdot \hat{\mathbf{x}}'\ ^2\}]$
H	$\frac{1}{4} [\mathcal{L}\{ \hat{\mathbf{x}} \cdot \hat{\mathbf{x}}'\ ^2\} + \mathcal{L}\{ \hat{\mathbf{y}} \cdot \hat{\mathbf{y}}'\ ^2\} + \mathcal{L}\{ \hat{\mathbf{x}} \cdot \hat{\mathbf{z}}'\ ^2\} + \mathcal{L}\{ \hat{\mathbf{y}} \cdot \hat{\mathbf{z}}'\ ^2\}]$
I	$\frac{3}{4} [\mathcal{L}\{ \hat{\mathbf{x}} \cdot \hat{\mathbf{x}}'\ ^2\} + \mathcal{L}\{ \hat{\mathbf{y}} \cdot \hat{\mathbf{y}}'\ ^2\}]$
J	$\frac{1}{4} [\mathcal{L}\{ \hat{\mathbf{x}} \cdot \hat{\mathbf{y}}'\ ^2\} + \mathcal{L}\{ \hat{\mathbf{y}} \cdot \hat{\mathbf{x}}'\ ^2\} + \mathcal{L}\{ \hat{\mathbf{x}} \cdot \hat{\mathbf{z}}'\ ^2\} + \mathcal{L}\{ \hat{\mathbf{y}} \cdot \hat{\mathbf{z}}'\ ^2\}]$

The various $\mathcal{L}\{|\hat{\mathbf{g}} \cdot \hat{\mathbf{g}}'|^2\}$ are evaluated using (9). For example

$$\begin{aligned} & \mathcal{L}\{|\hat{\mathbf{z}} \cdot \hat{\mathbf{y}}'|^2\} \\ &= \int_0^\infty \left| \sum_F \Phi_{zF} \Phi_{Fy'} \right|^2 \exp(-t/\tau) d(t/\tau), \\ &= \frac{1}{\tau} \int_0^\infty [-\sin \theta (\cos \theta \cos \dot{\phi} t \sin \dot{\chi} t + \sin \dot{\phi} t \cos \dot{\chi} t) \\ & \quad + \cos \theta (\sin \theta \sin \dot{\chi} t)]^2 \exp(-t/\tau) dt, \\ &= \frac{\sin^2 \theta (\cos^2 \theta + 1) \tau^2 [\dot{\phi}^2 + \dot{\chi}^2 + 4\tau^2 (\dot{\phi}^2 - \dot{\chi}^2)^2] + 4\dot{\phi} \dot{\chi} \tau^2 \cos \theta}{[1 + 4(\dot{\phi} + \dot{\chi})^2 \tau^2][1 + 4(\dot{\phi} - \dot{\chi})^2 \tau^2]} \\ & \quad + \frac{\sin^4 \theta \tau^2 (\dot{\phi}^2 - \dot{\chi}^2)}{(1 + 4\dot{\phi}^2 \tau^2)(1 + 4\dot{\chi}^2 \tau^2)} \\ & \quad - \frac{4 \sin^2 \theta \cos \theta [\tau^2 \dot{\chi}^2 \cos \theta (1 - 3\dot{\phi}^2 \tau^2 + 4\dot{\chi}^2 \tau^2) + \tau^2 \dot{\phi} \dot{\chi} (1 + \dot{\phi}^2 \tau^2)]}{[1 + \tau^2 (\dot{\phi} + 2\dot{\chi})^2][1 + (\dot{\phi} - 2\dot{\chi})^2 \tau^2](1 + \dot{\phi}^2 \tau^2)} \\ & \quad + \frac{2 \cos^2 \theta \sin^2 \theta \dot{\chi}^2 \tau^2}{(1 + 4\tau^2 \dot{\chi}^2)}. \quad (12) \end{aligned}$$

Using a similar procedure, $\mathcal{L}\{|\hat{\mathbf{z}} \cdot \hat{\mathbf{z}}'|^2\}$ and $\mathcal{L}\{|\hat{\mathbf{z}} \cdot \hat{\mathbf{x}}'|^2\}$ can be found (see table 4). It follows from (11) that for case *F*

$$\langle \cos^2 \gamma \rangle = \frac{1 + (\dot{\phi}\tau)^2(4 + \cos^2 \theta) + (\dot{\phi}\tau)^4(3 - 2 \cos^2 \theta + 3 \cos^4 \theta)}{2 + 10(\dot{\phi}\tau)^2 + 8(\dot{\phi}\tau)^4}. \quad (13)$$

In an analogous manner analytical expressions for $\langle \cos^2 \gamma \rangle$ can be derived for all the cases listed in table 1 using the results of tables 3 and 4. Then the polarization of the photofragment fluorescence is calculated from $\langle \cos^2 \gamma \rangle$ using either (3) or (4).

Equation (13) shows that $\langle \cos^2 \gamma \rangle$ in this case has no dependence on χ , the rate of precession of the *ABC** molecule about its figure axis. Indeed, the χ dependence vanishes except for cases *G*, *H*, *I* and *J*. Only in these cases does the precession rate of the molecular plane about the figure axis affect the average over the initial orientation of μ_{abs} and the final orientation of μ_{em} .

We summarize in table 5 the expressions for the polarization anisotropy $R = \frac{2}{3} \langle P_2(\cos \gamma) \rangle$ [see (4)] in the limit of direct photodissociation ($\tau \rightarrow 0$) and in the limit of slow predissociation ($\dot{\phi}\tau \rightarrow \infty$ and $\dot{\chi}\tau \rightarrow \infty$). The latter is of particular interest in the context of this study because resolved rotational structure in a predissociative transition is only expected under these conditions. Here it is seen that R is proportional to $[P_2(\cos \theta)]^2$ where $\cos^2 \theta = K^2/J(J+1)$. Thus $R=0$ when $\cos^2 \theta = \frac{1}{3}$ in which the figure axis of the *ABC** top makes the magic angle of 54.7° with respect to \mathbf{J} . We list in table 5 the values of R obtained when $\cos^2 \theta = 0$ ($K=0$) and $\cos^2 \theta = 1$ ($K=J$ for large J). For $K=J$ and $\tau \rightarrow \infty$, the polarization anisotropy is unaltered in cases *A-F* from its value for direct photodissociation ($\tau=0$). In these cases the rotational motion of the top cannot change the average angle μ_{em} makes with respect to μ_{abs} .

In the general case the value of R for $\tau=0$ differs from that for $\tau \rightarrow \infty$. For example, the cases *G* and *H* appear at first glance to be puzzling because the

Table 4. $\mathcal{L}\{|\hat{\mathbf{g}} \cdot \hat{\mathbf{g}}'|^2\} = \int_0^\infty |\hat{\mathbf{g}} \cdot \hat{\mathbf{g}}'|^2 \exp(-t/\tau) d(t/\tau)$ where the body-fixed g and g' frames are related to each other by the classical motion of a symmetric top.

$\hat{\mathbf{g}}$	$\hat{\mathbf{g}}'$	$\mathcal{L}\{ \hat{\mathbf{g}} \cdot \hat{\mathbf{g}}' ^2\}$
$\hat{\mathbf{x}}$	$\hat{\mathbf{x}}'$	$\frac{\cos^2 \theta (\cos^2 \theta + 1) [1 + 6\tau^2(\dot{\phi}^2 + \dot{\chi}^2) + 8\tau^4(\dot{\phi}^2 - \dot{\chi}^2)^2] - 8\tau^2 \dot{\phi} \dot{\chi} \cos^3 \theta}{2[1 + 4\tau^2(\dot{\phi} + \dot{\chi})^2][1 + 4\tau^2(\dot{\phi} - \dot{\chi})^2]}$ $- \frac{\sin^2 \theta \cos^2 \theta [1 + 2\tau^2(\dot{\phi}^2 + \dot{\chi}^2)]}{2(1 + 4\tau^2 \dot{\phi}^2)(1 + 4\tau^2 \dot{\chi}^2)}$ $+ \frac{2 \sin^2 \theta \cos^2 \theta [1 + 2\tau^2(\dot{\phi}^2 + 3\dot{\chi}^2) + \tau^4(\dot{\phi}^4 - 2\dot{\phi}^2 \dot{\chi}^2 + 8\dot{\chi}^4)] - 4\tau^2 \dot{\phi} \dot{\chi} \sin^2 \theta \cos \theta (1 + \tau^2 \dot{\phi}^2)}{[1 + \tau^2(\dot{\phi} + 2\dot{\chi})^2][1 + \tau^2(\dot{\phi} - 2\dot{\chi})^2](1 + \tau^2 \dot{\phi}^2)}$ $+ \frac{\sin^4 \theta (1 + 2\tau^2 \dot{\chi}^2)}{(1 + 4\tau^2 \dot{\chi}^2)}$
$\hat{\mathbf{x}}$	$\hat{\mathbf{y}}'$	$\frac{\tau^2 \cos^2 \theta (\cos^2 \theta + 1) [\dot{\phi}^2 + \dot{\chi}^2 + 4\tau^2(\dot{\phi}^2 - \dot{\chi}^2)^2] + 4\tau^2 \dot{\phi} \dot{\chi} \cos^3 \theta}{[1 + 4\tau^2(\dot{\phi} + \dot{\chi})^2][1 + 4\tau^2(\dot{\phi} - \dot{\chi})^2]}$ $+ \frac{\tau^2 \cos^2 \theta \sin^2 \theta (\dot{\phi}^2 - \dot{\chi}^2)}{(1 + 4\tau^2 \dot{\phi}^2)(1 + 4\tau^2 \dot{\chi}^2)}$ $+ \frac{4\tau^2 \cos \theta \sin^2 \theta [\dot{\chi}^2 \cos \theta (1 - 3\tau^2 \dot{\phi}^2 + 4\tau^2 \dot{\chi}^2) + \dot{\phi} \dot{\chi} (1 + \tau^2 \dot{\phi}^2)]}{[1 + \tau^2(\dot{\phi} + 2\dot{\chi})^2][1 + \tau^2(\dot{\phi} - 2\dot{\chi})^2](1 + \tau^2 \dot{\phi}^2)} + \frac{2\tau^2 \dot{\chi}^2 \sin^4 \theta}{(1 + 4\tau^2 \dot{\chi}^2)}$
$\hat{\mathbf{x}}$	$\hat{\mathbf{z}}'$	$\frac{6\tau^4 \dot{\phi}^4 \cos^2 \theta \sin^2 \theta}{(1 + 4\tau^2 \dot{\phi}^2)(1 + \tau^2 \dot{\phi}^2)}$
$\hat{\mathbf{y}}$	$\hat{\mathbf{x}}'$	$\frac{\tau^2 (\cos^2 \theta + 1) [\dot{\phi}^2 + \dot{\chi}^2 + 4\tau^2(\dot{\phi}^2 - \dot{\chi}^2)^2] + 4\tau^2 \dot{\phi} \dot{\chi} \cos \theta}{[1 + 4\tau^2(\dot{\phi} + \dot{\chi})^2][1 + 4\tau^2(\dot{\phi} - \dot{\chi})^2]} - \frac{\tau^2 \sin^2 \theta (\dot{\phi}^2 - \dot{\chi}^2)}{(1 + 4\tau^2 \dot{\phi}^2)(1 + 4\tau^2 \dot{\chi}^2)}$
$\hat{\mathbf{y}}$	$\hat{\mathbf{y}}'$	$\frac{(1 + \cos^2 \theta) [1 + 6\tau^2(\dot{\phi}^2 + \dot{\chi}^2) + 8\tau^4(\dot{\phi}^2 - \dot{\chi}^2)^2] - 8\tau^2 \dot{\phi} \dot{\chi} \cos \theta}{2[1 + 4\tau^2(\dot{\phi} + \dot{\chi})^2][1 + 4\tau^2(\dot{\phi} - \dot{\chi})^2]} + \frac{\sin^2 \theta [1 + 2\tau^2(\dot{\phi}^2 + \dot{\chi}^2)]}{2(1 + 4\tau^2 \dot{\phi}^2)(1 + 4\tau^2 \dot{\chi}^2)}$
$\hat{\mathbf{y}}$	$\hat{\mathbf{z}}'$	$\frac{2\tau^2 \dot{\phi}^2 \sin^2 \theta}{(1 + 4\tau^2 \dot{\phi}^2)}$
$\hat{\mathbf{z}}$	$\hat{\mathbf{x}}'$	$\frac{\sin^2 \theta (1 + \cos^2 \theta) [1 + 6\tau^2(\dot{\phi}^2 + \dot{\chi}^2) + 8\tau^4(\dot{\phi}^2 - \dot{\chi}^2)^2] - 8\tau^2 \dot{\phi} \dot{\chi} \cos \theta \sin^2 \theta}{2[1 + 4\tau^2(\dot{\phi} + \dot{\chi})^2][1 + 4\tau^2(\dot{\phi} - \dot{\chi})^2]}$ $- \frac{\sin^4 \theta [1 + 2\tau^2(\dot{\phi}^2 + \dot{\chi}^2)]}{2(1 + 4\tau^2 \dot{\phi}^2)(1 + 4\tau^2 \dot{\chi}^2)}$ $+ \frac{2 \sin^2 \theta \cos^2 \theta [1 + 2\tau^2(\dot{\phi}^2 + 3\dot{\chi}^2) + \tau^4(\dot{\phi}^4 - 2\dot{\phi}^2 \dot{\chi}^2 + 8\dot{\chi}^4)] - 4\tau^2 \dot{\phi} \dot{\chi} \sin^2 \theta \cos \theta (1 + \tau^2 \dot{\phi}^2)}{[1 + \tau^2(\dot{\phi} + 2\dot{\chi})^2][1 + \tau^2(\dot{\phi} - 2\dot{\chi})^2](1 + \tau^2 \dot{\phi}^2)}$ $+ \frac{\cos^2 \theta \sin^2 \theta (1 + 2\tau^2 \dot{\chi}^2)}{(1 + 4\tau^2 \dot{\chi}^2)}$
$\hat{\mathbf{z}}$	$\hat{\mathbf{y}}'$	$\frac{\tau^2 \sin^2 \theta (\cos^2 \theta + 1) [\dot{\phi}^2 + \dot{\chi}^2 + 4\tau^2(\dot{\phi}^2 - \dot{\chi}^2)^2] + 4\tau^2 \dot{\phi} \dot{\chi} \sin^2 \theta \cos \theta}{[1 + 4\tau^2(\dot{\phi} + \dot{\chi})^2][1 + 4\tau^2(\dot{\phi} - \dot{\chi})^2]}$ $+ \frac{\tau^2 \sin^4 \theta (\dot{\phi}^2 - \dot{\chi}^2)}{(1 + 4\tau^2 \dot{\phi}^2)(1 + 4\tau^2 \dot{\chi}^2)}$ $- \frac{4\tau^2 \sin^2 \theta \cos \theta [\dot{\chi}^2 \cos \theta (1 - 3\tau^2 \dot{\phi}^2 + 4\tau^2 \dot{\chi}^2) + \dot{\phi} \dot{\chi} (1 + \tau^2 \dot{\phi}^2)]}{[1 + \tau^2(\dot{\phi} + 2\dot{\chi})^2][1 + \tau^2(\dot{\phi} - 2\dot{\chi})^2](1 + \tau^2 \dot{\phi}^2)} + \frac{2\tau^2 \dot{\chi}^2 \cos^2 \theta \sin^2 \theta}{(1 + 4\tau^2 \dot{\chi}^2)}$
$\hat{\mathbf{z}}$	$\hat{\mathbf{z}}'$	$\frac{1 + \tau^2 \dot{\phi}^2 (3 + 2 \cos^2 \theta) + 2\tau^4 \dot{\phi}^4 (1 - 2 \cos^2 \theta + 3 \cos^4 \theta)}{(1 + 4\tau^2 \dot{\phi}^2)(1 + \tau^2 \dot{\phi}^2)}$

Downloaded by [Stanford University] at 10:52 13 July 2013

Table 5. The polarization anisotropy $R = \frac{2}{3} \langle P_2(\cos \theta) \rangle$ for direct photodissociation ($\tau=0$) and in the limit of slow predissociation ($\tau \rightarrow \infty$). For the column labelled $K=0$, $\cos \theta$ and χ are first set to zero and then the limit $\tau \rightarrow \infty$ is taken. Note that the column labelled General is not valid when $\cos \theta=0$ in cases G-J.

Case	R			
	$\tau=0$	$\tau \rightarrow \infty$		
		General	$K=0$	$K=J$
A	$\frac{2}{3}$	$\frac{2}{3} [P_2(\cos \theta)]^2$	$\frac{1}{10}$	$\frac{2}{3}$
B, C, E	$-\frac{1}{3}$	$-\frac{1}{3} [P_2(\cos \theta)]^2$	$-\frac{1}{20}$	$-\frac{1}{3}$
D, F	$\frac{1}{10}$	$\frac{1}{10} [P_2(\cos \theta)]^2$	$\frac{1}{20}$	$\frac{1}{10}$
G	$-\frac{1}{3}$	$\frac{1}{10} [P_2(\cos \theta)]^2$	$-\frac{1}{5}$	$\frac{1}{10}$
H	$\frac{1}{10}$	$-\frac{1}{20} [P_2(\cos \theta)]^2$	$\frac{1}{10}$	$-\frac{1}{20}$
I	$\frac{2}{3}$	$\frac{1}{10} [P_2(\cos \theta)]^2$	$\frac{1}{4}$	$\frac{1}{10}$
J	$-\frac{1}{3}$	$-\frac{1}{20} [P_2(\cos \theta)]^2$	$-\frac{1}{5}$	$-\frac{1}{20}$

value of R for $\tau=0$ changes sign from that for $\tau \rightarrow \infty$. This behaviour can be understood by examining what happens when $K=J$ ($\theta=0^\circ$ and z coincides with Z in figure 2 (a)). In case G μ_{abs} lies along \hat{x} while μ_{em} lies along \hat{y} at $\tau=0$; hence $\langle \cos^2 \gamma \rangle = 0$ and $R = -\frac{1}{5}$. As $\tau \rightarrow \infty$, the xz molecular plane rotates about the z axis, causing $\langle \cos^2 \gamma \rangle \rightarrow \frac{1}{2}$ and $R \rightarrow \frac{1}{10}$. In case H μ_{abs} has the same direction as in case G but μ_{em} is found to be uniformly distributed in the xz molecular plane. Hence at $\tau=0$, $\langle \cos^2 \gamma \rangle = \frac{1}{2}$ and $R = \frac{1}{10}$. As $\tau \rightarrow \infty$, μ_{abs} and μ_{em} lie uniformly distributed in two orthogonal planes, the xy plane for μ_{abs} and the xz plane for μ_{em} . Hence $\langle \cos^2 \gamma \rangle = \frac{1}{4}$ and $R = -\frac{1}{20}$. A comparison of the value of R at $\tau=0$ to that at $\tau \rightarrow \infty$ shows that the latter approaches more closely the value of zero, corresponding to an isotropic distribution of μ_{em} with respect to μ_{abs} . Finally, we note that individual rotational lines are often not resolved. Then an appropriate average of R , weighted by rotational line strengths, must be carried out [17].

This treatment could be generalized in a number of respects. For example, it applies to the dissociation of any planar parent molecule that yields an electronically excited symmetric top fragment. It is possible to consider the motion of an asymmetric top or to relax the assumption that the angular momentum of the fragment is perpendicular to the plane of the parent molecule. However, such treatments become very complex and will not be considered further here.

This work is supported by the U.S. National Science Foundation under NSF PHY 79-08694 and NSF CHE 80-17066.

REFERENCES

- [1] SIMONS, J. P., 1977, *Gas Kinetics and Energy Transfer* (Vol. 2, Chemical Society Specialist Periodical Report), pp. 56-95.
- [2] OKABE, H., 1978, *Photochemistry of Small Molecules* (John Wiley & Sons, Inc.).
- [3] VAN BRUNT, R. J., and ZARE, R. N., 1968, *J. chem. Phys.*, **48**, 4304.
- [4] ROTHE, E. W., KRAUSE, U., and DÜREN, R., 1980, *Chem. Phys. Lett.*, **72**, 100.
- [5] CHAMBERLAIN, G. A., and SIMONS, J. P., 1975, *Chem. Phys. Lett.*, **32**, 355.

- [6] CHAMBERLAIN, G. A., and SIMONS, J. P., 1975, *J. chem. Soc., Faraday II*, **71**, 2043.
- [7] MACPHERSON, M. T., and SIMONS, J. P., 1977, *Chem. Phys. Lett.*, **51**, 261.
- [8] MACPHERSON, M. T., and SIMONS, J. P., 1978, *J. chem. Soc., Faraday II*, **74**, 1965 ; 1979, *Ibid.*, **75**, 1572.
- [9] POLIAKOFF, E. D., SOUTHWORTH, S. H., SHIRLEY, D. A., JACKSON, K. H., and ZARE, R. N., 1979, *Chem. Phys. Lett.*, **65**, 407.
- [10] MACPHERSON, M. T., SIMONS, J. P., and ZARE, R. N., 1979, *Molec. Phys.*, **38**, 2049.
- [11] HUSAIN, J., WIESENFELD, J. R., and ZARE, R. N., 1980, *J. chem. Phys.*, **72**, 2479.
- [12] LOGE, G. W., and WIESENFELD, J. R., 1981, *Chem. Phys. Lett.*, **78**, 32.
- [13] FEOFILOV, P. P., 1961, *The Physical Basis of Polarized Emission* (Consultants Bureau Enterprises, Inc.).
- [14] MCCLINTOCK, M., DEMTRÖDER, W., and ZARE, R. N., 1969, *J. chem. Phys.*, **51**, 5509.
- [15] SYNGE, J. L., and GRIFFITH, B. A., 1959, *Principles of Mechanics* (McGraw-Hill Book Co., Inc.), pp. 374–383.
- [16] KING, G. W., HAINER, R. M., and CROSS, P. C., 1943, *J. chem. Phys.*, **11**, 27.
- [17] This is equivalent to averaging together different values of $\langle \cos^2 \gamma \rangle$ but *not* different values of P (as incorrectly done in Ref. [10]) because P does not depend linearly on $\langle \cos^2 \gamma \rangle$.